Convergence of threshold estimates for two-dimensional percolation

R. M. Ziff
Michigan Center for Theoretical Physics and Department of Chemical Engineering, University of Michigan, Ann Arbor, Michigan 48109-2136

M. E. J. Newman
Department of Physics, University of Michigan, Ann Arbor, Michigan 48109-1120
and Santa Fe Institute, 1399 Hyde Park Road, Santa Fe, New Mexico 87501

(Received 23 March 2002; published 29 July 2002)

Using a recently introduced algorithm for simulating percolation in microcanonical (fixed-occupancy) samples, we study the convergence with increasing system size of a number of estimates for the percolation threshold for an open system with a square boundary, specifically for site percolation on a square lattice. We show that the convergence of the average-probability estimate is described by a nontrivial correction-to-scaling exponent as predicted previously, and measure the value of this exponent to be 0.90 ± 0.02. For the median and cell-to-cell estimates of the percolation threshold we verify that convergence does not depend on this exponent, having instead a slightly faster convergence with a trivial analytic leading exponent.

DOI: 10.1103/PhysRevE.66.016129 PACS number(s): 64.60.Ak, 05.10.Ln, 05.70.Jk

I. INTRODUCTION

Percolation [1] is one of the most fundamental and widely studied systems in statistical physics. Theoretical studies of percolation models and applications of percolation theory to physical systems have spawned thousands of papers over the last few decades. Even so, there are some substantial gaps in our understanding of percolation. For example, we have at present no exact value for the position p_c of the percolation threshold for site percolation on that simplest of two-dimensional lattices, the square lattice. And in three dimensions we have almost no exact results whatsoever. Because of this, numerical methods have played an important role in the study of percolation. In this paper we consider a class of methods for estimating p_c for site percolation using finite-size scaling, and show how various estimates of p_c in this class scale with varying system size in two dimensions.

The methods studied here for measuring p_c are widely used and are all based upon consideration of the crossing probability function $R_L(p)$ [1–3]. This function gives the probability that a connected path crosses the system from one boundary segment to another, at site occupation probability p and system size or length scale L. Some examples of these estimates are the following.

(1) The renormalization-group (RG) fixed-point estimate $p_{\mathrm{RG}}(L) = p^*(L)$, where p^* is the solution to the equation [2,4]

$$R_L(p) = p. \tag{1}$$

(2) The average value of p at which crossing first occurs [1,2],

$$p_{\mathrm{av}}(L) = \langle p \rangle = \int_0^1 p R_L'(p)\, dp = 1 - \int_0^1 R_L(p)\, dp, \tag{2}$$

where the last equality follows from integrating by parts. The prime indicates differentiation with respect to p.

(3) The estimate $p_{R_c}(L)$ corresponding to the point where $R_L(p)$ equals its universal infinite-system value $R_c \equiv R_\infty(p_c)$ (which is determined by the system shape and boundary conditions) [5]:

$$R_L(p) = R_c. \tag{3}$$

For a square system, where $R_c = \frac{1}{2}$, this estimate $p_{0.5}(L)$ corresponds to the median of the distribution $R_L'(p)$. A related estimate $p_{h+v}(L)$ for rectangular systems is the value of p at which the horizontal and vertical crossing probabilities sum to unity [6–8]

$$R_L^{(h)}(p) + R_L^{(v)}(p) = 1. \tag{4}$$

This estimate is identical to $p_{R_c}(L) = p_{0.5}(L)$ when the boundary is a perfect square.

(4) The estimate $p_{\max}(L)$, which is the value of p where $R_L'(p)$ reaches a maximum [or equivalently, where $R_L(p)$ is at its inflection point] [2]:

$$R_L''(p) = 0. \tag{5}$$

(5) The cell-to-cell RG estimate, which is the point where two systems of different size have the same value of R [2]. One possible choice for this estimate, $p_{c\text{-}c}^{(1)}(L)$, is the value of p at which

$$R_L(p) = R_{L-1}(p), \tag{6}$$

while a second choice, $p_{c\text{-}c}^{(2)}(L)$, is the point at which

$$R_L(p) = R_{L/2}(p). \tag{7}$$

In order to use these estimates to determine the threshold precisely, we need to know the manner in which they converge to p_c as $L \to \infty$. While it is possible to simulate very large systems for which finite-size effects may be quite small, the statistics for such simulations are still relatively

poor because of the small number of samples that can typically be generated. In most cases, better results can be derived by doing more simulations on smaller systems, and this requires that the finite-size behavior is characterized accurately.

It is usually assumed (based upon very general scaling arguments) that all finite-system estimates of the percolation threshold converge to the bulk value p_c as

$$p_{\mathrm{est}}(L) - p_c \sim c L^{-1/\nu}, \tag{8}$$

where c is a system-dependent constant, and ν is the exponent governing the correlation length ξ, such that $\xi \sim |p - p_c|^{-\nu}$. (For the two-dimensional systems we will be looking at in this paper, $\nu = \frac{4}{3}$.) Well known exceptions to this behavior are a few highly symmetric, self-dual systems, such as bond percolation on a square lattice with a square boundary, and site percolation on a triangular lattice with a rhomboidal boundary; in both these cases $R_L(p)$ is perfectly symmetric about $p = \frac{1}{2}$ for all L and all the estimates above give $p_c = \frac{1}{2}$ exactly. For these systems, the constant c above is zero.

In Ref. [5], however, it was argued that for non-self-dual systems with a square boundary, such as site percolation on a square lattice (where because of the nonduality the estimates show finite-size effects), the convergence of most of the above estimates is faster than given by Eq. (8). This is an observation of some practical significance, since this particular system (site percolation on a square lattice with a square external boundary) is one of the most commonly studied systems in percolation. Similar arguments also apply to other symmetric two-dimensional crossing problems, such as a system with a rhomboidal boundary, which is commonly used when simulating triangular and honeycomb lattices.

The arguments of Ref. [5] were based upon the hypothesis that

$$R_L(p) \sim f_0(x) + L^{-1} f_1(x) + \cdots \tag{9}$$

for large L, where $x = (p - p_c) L^{1/\nu}$, $f_0(x)$ represents the universal part of R, and $f_1(x)$ represents the first-order correction to the scaling limit. The choice of L^{-1} as the leading order of the correction was based on numerical measurements of R at p_c, and can be derived from the assumption that the system is effectively slightly rectangular in shape, because of the different types of boundary conditions applied along the two principal axes [9]. For small x, it was assumed that

$$f_0(x) = a_0 + a_1 x + a_3 x^3 + \cdots, \tag{10}$$

$$f_1(x) = b_0 + b_1 x + b_2 x^2 + \cdots, \tag{11}$$

where $a_0 = \frac{1}{2}$ by the symmetry and self-duality of the square boundary. The same symmetry also implies that $f_0 - \frac{1}{2}$ is an odd function in x and hence that $a_n = 0$ for all even $n > 0$, as above. (To see that $f_0 - \frac{1}{2}$ is odd, note that for the perfectly dual system of bond percolation on a square lattice, $R - \frac{1}{2}$ is an odd function of x for all L, including $L = \infty$, and by universality, systems with other underlying lattices must behave the same way in the scaling limit.) In Ref. [5], no particular assumption was made about the behavior of $f_1(x)$, other than its analyticity about $x = 0$.

Note that the form of $f_0(x)$ in Eq. (10) is not entirely universal, because the independent variable x should incorporate a metric factor which depends upon the underlying lattice [10,11]. For convenience, however, since we are considering only one system of site percolation on a square lattice in this paper, we do not include that factor here.

Once the above assumptions, Eqs. (10) and (11), are made, the convergence of the various estimates of p_c is straightforward to analyze, and one finds that while the RG estimate does indeed converge according to Eq. (8) (a result that has been verified in many numerical studies), the rest of the estimates above should converge according to the faster behavior

$$p_{\mathrm{est}}(L) - p_c \sim c L^{-1-1/\nu}, \tag{12}$$

where the constant c varies from estimate to estimate. Simulations reported in Ref. [5] for systems of size up to 1024×1024 sites verified this convergence for the estimate $p_{0.5}$ to high accuracy. The estimates $p_{c\text{-}c}$, $p_{\max}$, and p_{av} were studied in Ref. [5] using only exact enumeration results for systems of sizes up to 7×7, which give polynomials for R (see the Appendix), and while the behavior of these results was found to be roughly consistent with Eq. (12), the uncertainty due to higher-order corrections was large.

Following the publication of Ref. [5], Hovi and Aharony [10,12] argued that the irrelevant scaling variables in the renormalization-group treatment of percolation imply a slower leading-order convergence of R_L to its infinite-system value, characterized by an exponent ω, whose value was deduced from the Monte Carlo work of Stauffer [13] to be about $\omega = 0.85$. (Note that Hovi and Aharony used θ_1 to denote the exponent we call ω.) A variety of series expansion results from the early 1980s were also analyzed to give values for this exponent ranging from 0.89 to over 1 [14,15].

The argument given by Hovi and Aharony implies that the leading terms in the expansion of $R_L(p)$ should in fact be

$$R_L(p) \sim f_0(x) + L^{-\omega} f_\omega(x) + L^{-1} f_1(x) + \cdots, \tag{13}$$

where

$$f_\omega(x) = c_1 x + c_2 x^2 + \cdots. \tag{14}$$

Hovi and Aharony argued that the constant term c_0 is zero for a square system, because at p_c there are no correction terms for the square-lattice, bond-percolation system, and corrections due to irrelevant variables should be universal. They also argued that $f_1(x)$ should be even, so that $b_1 = 0$ in Eq. (11), also by symmetry and self-duality. They discussed various consequences of these assumptions, and presented numerical evidence that the term containing the exponent ω is indeed the leading correction term, by showing that the behavior of $R_L(p)$ for large x (that is, for $p \neq p_c$) was better fit with such a term than without it. However, the procedure they used did not allow them to determine the value of ω accurately, because of the numerical difficulty of calculating

$R_L(p)$ precisely for all p. Furthermore, they did not study the convergence of the other estimates given above.

Recently [16,17], the present authors have shown that quantities such as $R_L(p)$ can be studied efficiently for all p by first finding the crossing probability $R_{L,n}$ in a microcanonical system of exactly n occupied sites, and then convolving with a binomial distribution to derive results for the corresponding canonical system thus:

$$R_L(p)=\sum_{n=0}^{N}\binom{N}{n}p^n(1-p)^{N-n}R_{L,n}, \tag{15}$$

where $N=L^2$ for site percolation on a square lattice. The microcanonical crossing probability is found using an efficient cluster-joining algorithm employing data structures based on trees, and a fast method is employed for checking for percolation on the fly during the progress of the calculation. (While many of the ideas incorporated in this method were put forward previously [18–23], to the best of our knowledge, this was the first time that all of these components were combined in this way, for the purpose of finding R efficiently. In Ref. [16] we studied the function corresponding to R for the probability of a cluster wrapping around the boundary of a periodic system on a torus. In the present paper, we describe how that method can be implemented for the crossing of an open system, and we report results from some large-scale simulations. The results allow us to determine accurately the behavior of all of the estimates above, and to test the theoretical predictions that follow from Eq. (13). As we will see, the appearance of the ''irrelevant'' term in the scaling of some estimates is confirmed, and a new, more precise value of ω is found.

The outline of the paper is as follows. In Sec. II we derive the expected scaling behavior of the various estimates of p_c, assuming the form of Eq. (13). In Sec. III we describe our numerical method, and in Sec. IV we present the results of our calculations. In Sec. V we give our conclusions.

II. CONVERGENCE OF ESTIMATES

If we assume Eq. (13) to be a correct description of the behavior of $R_L(p)$, it is straightforward to deduce the resulting convergence of the various estimates for p_c. In the following, we derive the leading correction term for each estimate, or the two leading terms when their powers are close to each other.

(1) The RG fixed point: The relevant terms of Eq. (1) are

$$\tfrac{1}{2}+a_1x+a_3x^3+\cdots=p_c+xL^{-1/\nu}, \tag{16}$$

which implies

$$p_{\mathrm{RG}}(L)=p_c+\left[\frac{p_c-\frac{1}{2}}{a_1}-\frac{a_3(p_c-\frac{1}{2})^3}{a_1^4}+\cdots\right]L^{-1/\nu}+O(L^{-2/\nu}). \tag{17}$$

The term in brackets is the value of x that is the solution to $f_0(x)=p_c$.

(2) Average-probability estimate: Equation (2) gives

$$p_{\mathrm{av}}(L)=1-L^{-1/\nu}\int_{x_0}^{x_1}[f_0(x)+L^{-\omega}f_\omega(x)+L^{-1}f_1(x)]dx, \tag{18}$$

where $x_0=-p_cL^{1/\nu}$ and $x_1=(1-p_c)L^{1/\nu}$, which are the values of x at $p=0$ and 1, respectively. Noting that, since $f_0(x)$ is odd about $f_0(0)=\frac{1}{2}$ and approaches 1 as $x\to\infty$, we have

$$L^{-1/\nu}\int_{x_0}^{x_1}f_0(x)dx\sim L^{-1/\nu}x_1=1-p_c, \tag{19}$$

we then get

$$p_{\mathrm{av}}(L)=p_c+L^{-\omega-1/\nu}\int_{-\infty}^{\infty}f_\omega(x)dx+L^{-1-1/\nu}\int_{-\infty}^{\infty}f_1(x)dx, \tag{20}$$

where we have extended the limits of the integrals to $\pm\infty$. This result is also implied by Eq. (40) of Ref. [12], for $n=1$. The order of the next correction depends upon the higher-order corrections to Eq. (13).

(3) Median-p estimate: Equation (3) gives

$$\tfrac{1}{2}+a_1x+b_0L^{-1}+c_1xL^{-\omega}+\cdots=\tfrac{1}{2}, \tag{21}$$

which implies

$$p_{0.5}(L)=p_c-\frac{b_0}{a_1}L^{-1-1/\nu}+O(L^{-1-\omega-1/\nu}). \tag{22}$$

(4) Maximum estimate: Equation (5) gives

$$6a_3x+2b_2L^{-1}+(2c_2+6c_3x)L^{-\omega}+\cdots=0, \tag{23}$$

which implies

$$p_{\max}(L)=p_c-\frac{c_2}{3a_3}L^{-\omega-1/\nu}-\frac{b_2}{3a_3}L^{-1-1/\nu}+O(L^{-2\omega-1/\nu}). \tag{24}$$

(5) Cell-to-cell estimate: Equation (6) gives

$$\begin{aligned}&a_0+a_1(p-p_c)L^{1/\nu}+b_0L^{-1}+c_1(p-p_c)L^{1/\nu-\omega}+\cdots\\&\quad=a_0+a_1(p-p_c)(L-1)^{1/\nu}+b_0(L-1)^{-1}\\&\qquad+c_1(p-p_c)(L-1)^{1/\nu-\omega}+\cdots,\end{aligned} \tag{25}$$

which implies

$$p_{c\text{-}c}^{(1)}(L)=p_c+\frac{b_0}{a_1}\nu L^{-1-1/\nu}+O(L^{-1-\omega-1/\nu}). \tag{26}$$

Likewise, for $p_{c\text{-}c}^{(2)}$ we have

$$p_{c\text{-}c}^{(2)}(L)=p_c+\frac{b_0}{a_1(1-2^{-1/\nu})}L^{-1-1/\nu}+O(L^{-1-\omega-1/\nu}). \tag{27}$$

Thus, the scaling of p_{RG}, $p_{0.5}$, and $p_{c\text{-}c}$ is unaffected to leading order by the presence of the exponent ω. However, p_{av} and $p_{\max}$ are affected by ω to leading order, scaling as $L^{-\omega-1/\nu}$, slightly slower than predicted in Ref. [5] (order $L^{-1-1/\nu}$). Note that b_1 does not enter in any of these results, so the leading scaling does not change if b_1 is equal to zero, as was argued to be the case in Ref. [12].

III. PROCEDURE

We have performed simulations to test the scaling hypotheses above using the algorithm described in Refs. [16,17]. Briefly, sites are occupied one by one in random order starting with an empty lattice. Occupied sites form contiguous clusters, each of which is identified uniquely by the site label of a chosen single site within the cluster, which we call the ''root site.'' Other (nonroot) sites within a cluster possess pointers that point either directly to the root site, or to other sites within the cluster such that by following a succession of pointers one can get from any site to the root. A newly added site is considered to be a cluster of size 1, which is its own root site, and bonds are then added between it and any adjacent occupied sites. The clusters to which sites at either end of such a bond belong are identified by following pointers from them to their corresponding root sites, and if the root sites found are different we conclude that two different clusters have been joined by the addition of the bond. We represent this by adding a pointer from the root site of one of the clusters to the root site of the other. Smaller clusters are always made subclusters of larger ones, and all pointers followed are subsequently changed to point directly to the root of their own cluster. The net result is an algorithm that can calculate $R_{L,n}$ (and many other observable quantities) for all values of n in average running time which is of order the area of the lattice, or $O(L^2)$ for a square lattice.

In our previous calculations using this algorithm we measured the probability of the existence of a cluster that wraps around the periodic boundary conditions of a toroidal lattice. In this paper we are interested instead in the existence (or not) of a cluster that spans an open system along one given direction. There are (at least) three efficient methods for detecting spanning of this kind, two of which are described in detail in Ref. [17] and all of which we have used in the present work. In the first method, we use the same pointer-based trick that we used in Ref. [16] to detect wrapping with periodic boundary conditions, but start out with an $(L+1)\times(L+1)$ lattice in which one horizontal row of sites is fixed to be permanently empty and one vertical one is fixed occupied. Occurrence of a wrapping cluster in such a system is then exactly equivalent to the occurrence of a spanning cluster in the horizontal direction in an open system with dimensions $L\times L$.

In the second method, two complete rows of sites at the top and bottom of an open $(L+2)\times(L+2)$ lattice are fixed permanently empty, and two columns of L sites on the left and the right sides of the lattice are fixed occupied. The two columns of occupied sites form two initial clusters on the lattice. By following pointers from one site in each of these clusters it is then simple to determine whether the two clusters have been amalgamated by other sites added between them: if they have the same root site they have been amalgamated, otherwise they have not. Performing this check after the addition of each site to the lattice, we can detect when a spanning cluster on the $L\times L$ open lattice first appears. The two methods have comparable running times and give compatible results. The second is somewhat simpler to implement.

In the third method, which was used for the majority of the simulations here, we consider an $L\times L$ open lattice and keep track of the minimum and maximum x and y coordinates for sites in each cluster, updating their values as necessary when clusters are joined. When $x_{\max}-x_{\min}=L-1$ for a cluster, we know that the cluster spans the lattice in the horizontal direction, and similarly for vertical crossing. This method allows one to check for both crossing events simultaneously, and it is also efficient and easy to program. A similar method was used in Ref. [24] for simulations of the Ising model.

Since in the present calculation we are interested only in the existence or not of a system-spanning cluster, we can stop the simulation once a spanning cluster is detected, as spanning must also occur for all higher values of n. This produces about a 40% saving in running time. Each simulation then produces just a single number, the value of n at which a spanning cluster first appears (or two numbers if we check for spanning in both the horizontal and vertical directions). Making a histogram of these values over many runs of the algorithm, we derive an estimate of the probability $P_{L,n}$ that the system first percolates when the number of occupied sites reaches n. This probability is related to the desired function $R_{L,n}$ according to $P_{L,n}=R_{L,n}-R_{L,n-1}$, and hence

$$R_{L,n}=\sum_{n'=0}^{n} P_{L,n'}. \tag{28}$$

Once the $R_{L,n}$ is determined, $R_L(p)$, the corresponding function in the canonical percolation ensemble, is calculated from Eq. (15), with the binomial coefficients for large N being calculated by iterative multiplication [17]. The estimates p_{RG}, $p_{0.5}$, and $p_{c\text{-}c}$ for the percolation threshold are then evaluated directly according to Eqs. (2), (3), and (6). The estimate, p_{av}, could be found directly by performing a numerical integral over $R_L(p)$, but a better method is to use the following exact formula:

$$\begin{aligned} p_{\mathrm{av}} &= 1-\int_0^1 R_L(p)\,dp \\ &= 1-\sum_{n=0}^{N}\binom{N}{n}R_{L,n}\int_0^1 p^n(1-p)^{N-n}\,dp \\ &= 1-\frac{1}{N+1}\sum_{n=0}^{N} R_{L,n}. \end{aligned} \tag{29}$$

Using Eq. (28) this can also be written directly in terms of $P_{L,n}$ as

TABLE I. Various estimates of p_c from the simulations ($L \geqslant 7$), where N_S is the number of samples, and from exact expressions ($L \leqslant 7$). The cell-to-cell estimate is $p_{c\text{-}c}^{(1)}$ for superscript (1) and $p_{c\text{-}c}^{(2)}$ for superscript (2). Errors in the numerical results are generally in the last digit quoted.

L	N_S	p_{RG}	$p_{\mathrm{av}}=\langle p\rangle$	$p_{0.5}$	$p_{c\text{-}c}$	$p_{\max}$	$\sqrt{\langle(\Delta p)^2\rangle}$	$R_L(p_c)$
2	(exact)	0.618 033 99	0.533 333 33	0.541 196 10		0.577 350 27	0.221 108 32	0.579 250 7
3	(exact)	0.619 260 13	0.552 380 95	0.559 296 32	0.620 734 47$^{(1)}$	0.580 302 37	0.181 379 08	0.566 703 6
4	(exact)	0.619 355 42	0.564 009 19	0.569 724 13	0.619 583 78$^{(1)}$	0.584 399 52	0.154 834 66	0.555 588 4
5	(exact)	0.618 095 29	0.571 145 67	0.575 810 07	0.613 506 05$^{(1)}$	0.586 759 48	0.135 844 2	0.547 538 4
6	(exact)	0.616 587 09	0.575 850 67	0.579 702 76	0.609 208 76$^{(1)}$	0.588 256 53	0.121 512 46	0.541 467 0
7	(exact)	0.615 117 36	0.579 119 47	0.582 351 30	0.606 075 99$^{(1)}$	0.589 265 61	0.110 272 24	0.536 751 3
7	1.0×10^{10}	0.615 118 0	0.579 120 4	0.582 351 9	0.606 081 2$^{(1)}$	0.589 265 5	0.110 272 0	0.536 749
8	6.0×10^{9}	0.613 765 6	0.581 486 6	0.584 239 4	0.608 314$^{(2)}$	0.589 975 5	0.101 192 5	0.532 998
16	2.0×10^{9}	0.606 902 2	0.588 781 9	0.589 885 8	0.598 828$^{(2)}$	0.592 010 4	0.063 376 1	0.518 117
32	2.0×10^{9}	0.601 631 9	0.591 424 6	0.591 835 2	0.594 825$^{(2)}$	0.592 602 6	0.038 720 3	0.509 535
64	3.0×10^{9}	0.598 148 5	0.592 317 9	0.592 465 7	0.593 413$^{(2)}$	0.592 739 1	0.023 337 9	0.504 890
128	1.0×10^{9}	0.595 983 7	0.592 608 7	0.592 661 3	0.592 952$^{(2)}$	0.592 757 7	0.013 970 3	0.502 476
256	4.0×10^{8}	0.594 674 2	0.592 701 3	0.592 720 8	0.592 808$^{(2)}$	0.592 753 6	0.008 334 3	0.501 24

$$p_{\mathrm{av}}=1-\frac{1}{N+1}\sum_{n=0}^{N}\sum_{n'=0}^{n}P_{L,n'}=\frac{1}{N+1}\sum_{n=0}^{N}nP_{L,n}, \tag{30}$$

which means that the canonical average position of the percolation threshold is $N/(N+1)$ times the microcanonical average $(1/N)\Sigma nP_{L,n}$ and no convolution is necessary to find its value. Higher moments of the distribution R' can be found in a similar fashion. For the second moment, for example, we have

$$\langle p^2\rangle=\int_0^1 p^2R_L'(p)dp=1-\frac{2}{(N+1)(N+2)}\sum_{n=0}^{N}(n+1)R_{L,n}$$
$$=\frac{1}{(N+1)(N+2)}\sum_{n=0}^{N}n(n+1)P_{L,n}. \tag{31}$$

To find where $R_L''(p)=0$ for the estimate $p_{\max}$, we make use of the following result:

$$R_L''(p)=\sum_{n=0}^{N}\binom{N}{n}p^n(1-p)^{N-n}R_{L,n}$$
$$\times\left[\frac{n(n-1)}{p^2}-\frac{2n(N-n)}{p(1-p)}+\frac{(N-n)(N-n+1)}{(1-p)^2}\right]. \tag{32}$$

The above three results, along with Eq. (15), demonstrate further the advantage of calculating $R_L(p)$ through the microcanonical $R_{L,n}$: quantities such as $R_L(p)$ and $R_L''(p)$ can be calculated exactly at all p, while p_{av} can be found without introducing any error through numerical integration.

In the more familiar binary search method for finding $R_L(p)$ [1], p is increased or decreased to narrow the bounds on one's estimate of the position of the percolation point for a given realization of the disorder. This search process is stopped after some number m of iterations, typically about 15, giving a resolution of 2^{-m} on the estimate for p_c. Thus, $R_L(p)$ is evaluated at only a finite set of points, and this adds some uncertainty to the calculation, beyond the basic statistical error. Given that our microcanonical method is also much faster than binary search due to its efficient cluster merging and percolation checking, there seems no reason to use other methods when quantities such as $R_L(p)$ are desired for a range of values of p.

IV. RESULTS OF SIMULATIONS

Simulations were carried out for $L=7,8,16,32,64,128,256$. The results are given in Table I, along with exact results from exhaustive enumeration of states for small systems with $L\leqslant7$. The polynomials from which the exact results are derived are listed in the Appendix. We conducted the simulations at $L=7$ to compare numerical and exact results, and the agreement was found to be perfect within the statistical accuracy of the simulations. The pseudorandom number generator used for the simulations was the four-tap feedback generator known as R9689 or GFSR4 [25].

An error analysis for the simulation data indicates that the estimates of p_c are accurate to about six figures, and the values of $R(p_c)$ are accurate to four or five figures, as indicated in the table. We also simulated 2.4×10^7 samples for a system of size $L=512$, but the statistical accuracy of the results was insufficient to add anything to the present analysis.

Consider the results for the estimate $p_{\max}$, whose convergence is nonmonotonic. Its value starts below p_c for small systems, then goes above p_c as the lattice size passes through $L\simeq100$, and presumably converges to p_c from above as $L\to\infty$. Indeed, according to Eq. (24), $p_{\max}$ has two correction terms with closely spaced scaling exponents $-\omega-1/\nu\approx-1.65$ (using the value of ω from below) and $-1-1/\nu=-1.75$; it appears that these terms contribute more or less equally in the range of system sizes that we are considering.

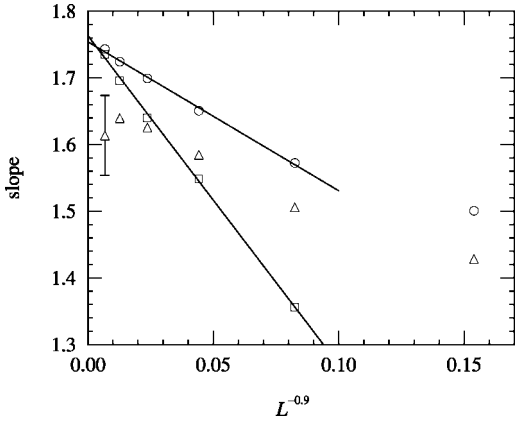

FIG. 1. Absolute values of the pairwise slopes $-[\ln|p_{\rm est}(L)-p_c|-\ln|p_{\rm est}(\frac{1}{2}L)-p_c|]/\ln 2$, plotted as a function $L^{-\omega}$, for the estimates $p_{0.5}(L)$ (circles), $p_{\rm av}(L)$ (triangles), and $p^{(2)}_{c\text{-}c}(L)$ (squares) with $p_c=0.592\,746\,2$.

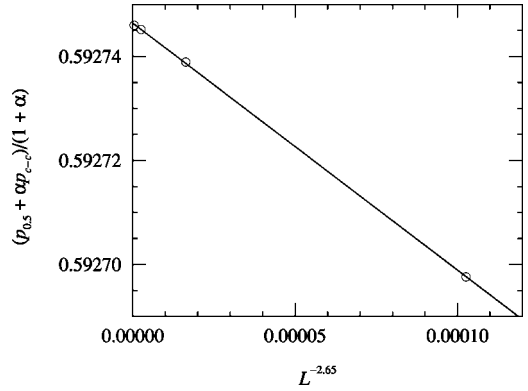

FIG. 2. Plot of $(p_{0.5}+\alpha p^{(2)}_{c\text{-}c})/(1+\alpha)$ vs $L^{-2.65}$, where $\alpha=1-2^{-1/\nu}$.

The observed behavior is consistent with Eq. (24) if $b_2<0$, $c_2>0$, and the two are roughly comparable in magnitude. [Note that $a_3<0$ because $f_0'(x)$ is at a maximum at $x=0$.] It is not possible to fit the exponents of Eq. (24) reliably to these data.

The rest of the estimates are all monotonic, and lead to reasonably straight lines when viewed on a logarithmic plot of $|p_{\rm est}-p_c|$ vs L, reflecting the leading power-law behavior. To provide a more sensitive representation of our data, we calculate successive (negative) slopes between pairs of points for systems of sizes $\frac{1}{2}L$ and L, $-[\ln|p_{\rm est}(L)-p_c|-\ln|p_{\rm est}(\frac{1}{2}L)-p_c|]/\ln 2$ for the various estimates $p_{\rm est}(L)$. For these calculations we used the value $p_c=0.592\,746\,2$ given in Ref. [16], which is consistent with the data presented here, but of somewhat higher precision than these data would yield.

In Fig. 1 we show the plots of the successive slopes for estimates $p_{0.5}(L)$, $p^{(2)}_{c\text{-}c}(L)$, and $p_{\rm av}(L)$, as a function of $L^{-\omega}$ with $\omega=0.9$. According to Eqs. (22) and (27), both of these estimates should converge with a leading exponent of $-1-1/\nu$ and a next-order term of order $-1-1/\nu-\omega$, which implies that the successive slopes should fall on a straight line when plotted as a function of $L^{-\omega}$, with an intercept of 1.75. This behavior is indeed seen in Fig. 1, with measured intercepts of 1.754 and 1.763, respectively. (Note that agreement is not highly sensitive to the value of ω; if the data were plotted as a function of L^{-1}, the fit to linearity would not be much worse.)

The successive slopes for $p_{\rm av}(L)$ do not fall on as good a straight line as the other estimates, presumably because the exponents $-\omega-1/\nu$ and $-1-1/\nu$ of the two leading terms in convergence are closely spaced [see Eq. (20)]. Extrapolation to $L=\infty$ is still possible however, and we find an intercept at $1/\nu+\omega=1.65\pm0.02$, clearly different from the value of 1.75 for the other estimates, implying $\omega=0.90\pm0.02$, the figure we have used above. The error bars are smaller than the size of the symbols for all L except $L=256$, as shown in the plot. Although ω is used in the abscissa of Fig. 1, its value there has little effect on the determination of ω from the intercept of $p_{\rm av}(L)$.

We can also compare the coefficients for the leading behavior of estimates to their predicted values. For example, the predicted value of the leading coefficient for $p_{0.5}$, Eq. (22), is $b_0/a_1=0.423$, using values of $b_0=0.322$ (see below) and $a_1=0.765$ [5,12]. This compares favorably with the value measured here of 0.436. And for $p^{(2)}_{c\text{-}c}$, the coefficient from Eq. (27), $b_0/[a_1(1-2^{-1/\nu})]$, should have a value of 1.04, which compares favorably with the measured value 1.02. Note that if we take the linear combination of these two estimates (whose finite-size corrections are opposite in sign), $(p_{0.5}+\alpha p^{(2)}_{c\text{-}c})/(1+\alpha)$, where $\alpha=1-2^{-1/\nu}$, the leading correction terms are predicted to cancel one another and the combination should have leading scaling of $L^{-1-\omega-1/\nu}=L^{-2.65}$. And indeed this combination is seen to converge very quickly in our numerical results, with values 0.592 698, 0.592 739, 0.592 745, and 0.592 746 for $L=32$, 64, 128, and 256, respectively. The plot of these figures vs $L^{-2.65}$ given in Fig. 2 shows linear behavior as expected, with an intercept at $p=0.592\,746\,4(5)$, consistent with the best current figure of $p_c=0.592\,746\,2(1)$ [16]. Thus, by taking a combination of estimates, we can improve the convergence rate for the open system to the point where it becomes competitive with that of the periodic system, in which the estimate with the best convergence has the exponent $-11/4$ [16]. This cancellation of leading-order corrections between the two terms is expected to be universal.

The results for $p_{\rm RG}-p_c$ and the standard deviation $\sigma=\sqrt{\langle(\delta p)^2\rangle}=\sqrt{\langle p^2\rangle-\langle p\rangle^2}$ converge to zero with the predicted exponent $-1/\nu=-0.75$ [see Eq. (8)], as demonstrated in Fig. 3, where we plot the (negative) successive slopes as a function of $1/L$. The latter represents expected higher-order scaling of these estimates. The intercepts of these curves (which give the negative of the scaling exponent) are at 0.749 and 0.763, respectively. The prediction that σ converges as $L^{-1/\nu}$ is given in Ref. [12] and also follows from the equations of Sec. II.

We also show in Fig. 4 a plot of the type introduced by Stauffer, in which $p_{\rm RG}$ is shown as a function of σ, allowing extrapolation to infinite system size to be carried out without knowledge of the value of ν [1]. This plot shows nearly

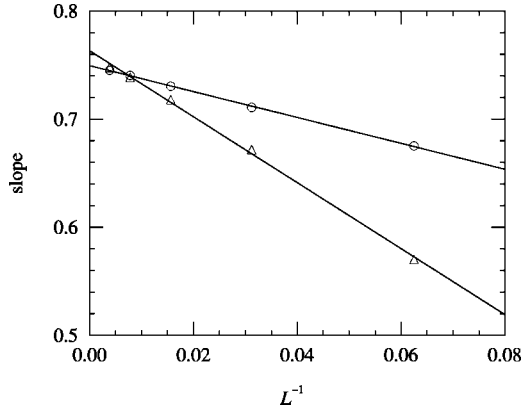

FIG. 3. Absolute values of the pairwise slopes of $-[\ln|p_{\mathrm{RG}}(L)-p_c|-\ln|p_{\mathrm{RG}}(L/2)-p_c|]/\ln 2$, with $p_c=0.592\,746\,2$ (triangles), and of the standard deviation of the distribution of p (circles), plotted as a function L^{-1}. The lines are fit through all the points.

linear behavior, with the last three points ($L=64$, 128, and 256) well fit by the line $p_{\mathrm{RG}}=0.592\,746\,5+0.231\,512\sigma$ with $R^2=0.999\,997\,9$. The intercept is in excellent agreement with the known value of p_c, although this high agreement is perhaps somewhat fortuitous, considering the slow convergence of the RG estimate.

The last column of Table I gives the crossing probability at p_c. The considerations in Sec. II imply that $R_L(p_c)\sim 1/2+b_0/L$ with no contributions from the irrelevant scaling variable [5,12,26], and indeed an analysis of these data shows good agreement with the behavior $R_L(p_c)=1/2+0.320/L-0.44/L^2+\cdots$, yielding $b_0=0.320\pm 0.001$. This is nearly identical to the value 0.319 given in Ref. [5] (where larger systems, but with lower statistics, were generated) and the value 0.31 ± 0.01 of Ref. [12].

Besides the results presented here, the data on the microcanonical crossing functions can be used to study additional properties of $R(p)$. For example, the derivative $R'(p)$ may be calculated by a formula similar to Eq. (32), and according to Eq. (13) this quantity should scale as $L^{-1/\nu}R'(p_c)=a_1+c_1L^{-\omega}$ at p_c (with no contribution of order L^{-1}). Plotting the results of $L^{-1/\nu}R'(p_c)$ against $L^{-\omega}$ for $L=16$–256, and

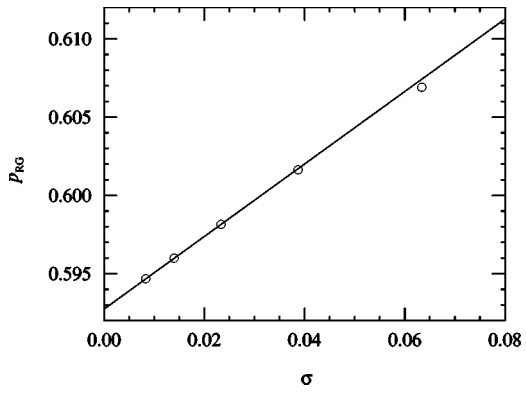

FIG. 4. "Stauffer plot" of p_{RG} vs $\sigma=\sqrt{\langle(\Delta p)^2\rangle}$; the line is fit through the leftmost three points and its equation is given in the text.

TABLE II. Exact results for $R_L(p)$ expressed as polynomials in p, for $L=2$ to 7.

L	$R_L(p)$
2	$2p^2-p^4$
3	$3p^3+4p^4-6p^5-9p^6+14p^7-6p^8+p^9$
4	$4p^4+12p^5-6p^6-28p^7-22p^8+48p^9+66p^{10}-108p^{11}+10p^{12}+44p^{13}-20p^{14}+p^{16}$
5	$5p^5+24p^6+12p^7-62p^8-92p^9-41p^{10}+274p^{11}+42p^{12}+474p^{13}-1336p^{14}+172p^{15}-197p^{16}+4791p^{17}-9015p^{18}+8013p^{19}-4261p^{20}+1559p^{21}-450p^{22}+103p^{23}-15p^{24}+p^{25}$
6	$6p^6+40p^7+60p^8-80p^9-248p^{10}-276p^{11}+201p^{12}+944p^{13}-298p^{14}+2392p^{15}-2420p^{16}+548p^{17}-24\,848p^{18}+38\,688p^{19}-7540p^{20}+515\,64p^{21}-117\,312p^{22}-133\,312\,p^{23}+588\,639\,p^{24}-608\,464\,p^{25}+683\,62p^{26}+420\,396\,p^{27}-455\,910\,p^{28}+235\,816\,p^{29}-62\,454p^{30}+3200p^{31}+3212p^{32}-1024p^{33}+120p^{34}-p^{36}$
7	$7p^7+60p^8+150p^9-18p^{10}-490p^{11}-885p^{12}-318p^{13}+1464p^{14}+3056p^{15}-1586p^{16}+5584p^{17}-6520p^{18}+43\,150p^{19}-153\,589\,p^{20}+128\,504\,p^{21}-407\,257\,p^{22}+127\,828\,8p^{23}-124\,319\,3p^{24}+219\,537\,4p^{25}-698\,363\,0p^{26}+827\,153\,6p^{27}-699\,066\,9p^{28}+177\,413\,31p^{29}-113\,444\,31p^{30}-552\,949\,29p^{31}+916\,429\,05p^{32}+671\,521\,94p^{33}-374\,255\,572\,p^{34}+557\,174\,473\,p^{35}-463\,108\,229\,p^{36}+225\,338\,948\,p^{37}-471\,353\,60p^{38}-129\,506\,91p^{39}+111\,688\,48p^{40}-172\,480\,4p^{41}-106\,730\,5p^{42}+689\,318\,p^{43}-196\,565\,p^{44}+34\,848p^{45}-4391p^{46}+422p^{47}-28p^{48}+p^{49}$

adjusting ω to get the best linear regression, we find an excellent fit ($R^2=0.999\,985$) with $\omega=0.8891$, $a_1=0.7616$, and $c_1=0.3555$. This value of ω is consistent with the results above. The value of a_1 is slightly below the value $a_1=0.765$ found previously [5,12]; this difference can be attributed to the extrapolation to infinity done here [for example, at $L=256$, the value of $L^{-1/\nu}R'(p_c)$ is equal to 0.7842]. Many other results can be extracted in a similar fashion once we have numerical data for the microcanonical $R_{L,n}$.

V. CONCLUSIONS

We have studied the finite-size scaling of estimates of the percolation threshold p_c derived from the crossing probability $R_L(p)$ for site percolation on the square lattice. Our numerical results confirm that different estimates converge to p_c with a variety of scaling exponents as predicted by the scaling theory developed in Refs. [5,10,12]. In particular, we have shown that the average threshold estimate p_{av} converges with a nontrivial exponent $L^{-\omega-1/\nu}$, whose origins lie in the irrelevant variables in the renormalization-group treatment of the problem, and our results for this estimate provide us with a direct measurement of that exponent. We find $\omega=0.90\pm 02$, somewhat higher than the value of about 0.85

TABLE III. Exact results for $R_L(p,q)$ expressed as polynomials in p and $q \equiv 1-p$, for $L=2$ to 7.

L	$R_L(p,q)$
2	$2p^2q^2+4p^3q+p^4$
3	$3p^3q^6+22p^4q^5+59p^5q^4+67p^6q^3+36p^7q^2+9p^8q+p^9$
4	$4p^4q^{12}+60p^5q^{11}+390p^6q^{10}+1452p^7q^9+3416p^8q^8+5272p^9q^7+5414p^{10}q^6+3736p^{11}q^5$ $+1752p^{12}q^4+560p^{13}q^3+120p^{14}q^2+16p^{15}q+p^{16}$
5	$5p^5q^{20}+124p^6q^{19}+1418p^7q^{18}+9958p^8q^{17}+48\,171p^9q^{16}+170\,391p^{10}q^{15}+456\,051p^{11}q^{14}$ $+942\,077p^{12}q^{13}+151\,813\,3p^{13}q^{12}+191\,788\,7p^{14}q^{11}+190\,335\,9p^{15}q^{10}+148\,630\,8p^{16}q^9$ $+915\,643p^{17}q^8+446\,538p^{18}q^7+172\,749p^{19}q^6+52\,871p^{20}q^5+12\,650p^{21}q^4+2300p^{22}q^3$ $+300p^{23}q^2+25p^{24}q+p^{25}$
6	$6p^6q^{30}+220p^7q^{29}+3830p^8q^{28}+42\,200p^9q^{27}+330\,862p^{10}q^{26}+196\,683\,2p^{11}q^{25}+922\,005\,1p^{12}q^{24}$ $+349\,865\,68p^{13}q^{23}+109\,429\,240p^{14}q^{22}+285\,726\,952p^{15}q^{21}+628\,339\,894p^{16}q^{20}$ $+117\,065\,617\,2p^{17}q^{19}+185\,451\,985\,6p^{18}q^{18}+250\,279\,719\,2p^{19}q^{17}+287\,954\,750\,7p^{20}q^{16}$ $+282\,477\,386\,8p^{21}q^{15}+236\,295\,381\,8p^{22}q^{14}+168\,645\,572\,0p^{23}q^{13}+102\,808\,519\,7p^{24}q^{12}$ $+536\,110\,144p^{25}q^{11}+239\,427\,498p^{26}q^{10}+915\,847\,20p^{27}q^9+299\,432\,38p^{28}q^8$ $+832\,262\,0p^{29}q^7+194\,684\,2p^{30}q^6+376\,992p^{31}q^5+58\,905p^{32}q^4+7140p^{33}q^3+630p^{34}q^2$ $+36p^{35}q+p^{36}$
7	$7p^7q^{42}+354p^8q^{41}+8637p^9q^{40}+135\,542p^{10}q^{39}+153\,891\,8p^{11}q^{38}+134\,800\,33p^{12}q^{37}$ $+948\,508\,47p^{13}q^{36}+551\,119\,224p^{14}q^{35}+269\,732\,922\,5p^{15}q^{34}+112\,862\,456\,29p^{16}q^{33}$ $+408\,335\,758\,12p^{17}q^{32}+128\,871\,332\,816p^{18}q^{31}+357\,226\,485\,246p^{19}q^{30}$ $+874\,366\,412\,699p^{20}q^{29}+189\,748\,991\,302\,9p^{21}q^{28}+366\,204\,287\,877\,7p^{22}q^{27}$ $+629\,886\,980\,328\,3p^{23}q^{26}+966\,956\,844\,729\,7p^{24}q^{25}+132\,585\,068\,442\,89p^{25}q^{24}$ $+162\,424\,120\,333\,36p^{26}q^{23}+177\,768\,801\,987\,90p^{27}q^{22}+173\,788\,593\,629\,74p^{28}q^{21}$ $+151\,728\,375\,886\,87p^{29}q^{20}+118\,300\,132\,565\,60p^{30}q^{19}+823\,920\,775\,762\,1p^{31}q^{18}$ $+512\,857\,828\,295\,4p^{32}q^{17}+285\,516\,297\,755\,8p^{33}q^{16}+142\,265\,267\,827\,2p^{34}q^{15}$ $+634\,745\,588\,151p^{35}q^{14}+253\,562\,760\,568p^{36}q^{13}+905\,980\,448\,53p^{37}q^{12}+288\,886\,115\,91p^{38}q^{11}$ $+818\,938\,813\,8p^{39}q^{10}+205\,207\,815\,2p^{40}q^9+450\,849\,373p^{41}q^8+858\,971\,97p^{42}q^7$ $+139\,838\,16p^{43}q^6+190\,688\,4p^{44}q^5+211\,876p^{45}q^4+18424p^{46}q^3+1176p^{47}q^2$ $+49p^{48}q+p^{49}$

found previously [13] but consistent with the (wide) bounds set by series studies [14,15]. Our result is in good agreement with a renormalization-group result of $\omega=0.915$ found by Burkhardt [27,32]. More extensive simulations could be done to give ω to higher precision.

Of the estimates considered here, p_{av} is the only one that shows the effect of the irrelevant exponent clearly. The estimates $p_{0.5}$ and $p_{c\text{-}c}$ are confirmed to converge as $L^{-1-1/\nu}$, as proposed previously [5]. The maximum estimate $p_{\max}$ is found to exhibit nonmonotonic behavior, which can be explained by competition between correction terms with closely spaced exponents $-1-1/\nu$ and $-\omega-1/\nu$.

The numerical results reported here were found using a microcanonical simulation method, which allows one to calculate $R_L(p)$ easily for any p [16,17]. The various estimates can then be found quickly to any desired degree of precision by applying appropriate formulas, Eqs. (1)–(7). This method proves to be particularly advantageous for the estimate p_{av}, since this estimate depends on knowing $R_L(p)$ for all values of p, the determination of which by most other methods requires a great deal of work. From the microcanonical data, p_{av} can be found without any calculational bias using Eq. (30).

Having characterized the convergence rates of our various threshold estimates, one can go back to older literature and find many instances where an anomalous rate of convergence was seen but not fully understood or recognized. For example, Reynolds *et al.* [2] derived an estimate of p_c which is equivalent to our p_{av} from numerical data for the one-way crossing probability, which they denoted R_1. Assuming this estimate to scale as Eq. (8), they plotted their results against $L^{-1/\nu}$ (their Fig. 13). The resulting plot is seen to fall on a nearly vertical line, consistent with higher-order behavior. Fitting their data with the supposed $L^{-1/\nu}$ scaling, they deduced a best estimate of $p_c=0.5931$ in the large system-size limit. If however one assumes instead the $L^{-\omega-1/\nu}$ scaling predicted by the theory [10,12], the intercept of their data becomes $p_c \simeq 0.5927$, which is much closer to the current best estimate of this quantity.

Yonezawa *et al.* [6] plotted a quantity essentially equivalent to our $p_{0.5}$ as a function of $L^{-1/\nu}$, and found apparent agreement with this assumed L dependence (their Figs. 7 and 8). The expected $L^{-1-1/\nu}$ behavior is evidently too weak to be distinguished from $L^{-1/\nu}$ within the errors on their numerical data. Similarly, Hu *et al.* [28] believed the cell-to-cell estimate $p_{c\text{-}c}^{(1)}$ to be insensitive to L; again, the precision of their work did not allow them to observe the higher-order scaling predicted by Eq. (27).

It should be emphasized that the convergence behavior discussed here is specific to a two-dimensional system with a square or rhomboidal open boundary, with the crossing de-

fined as a path from one specified side to its opposite. Because of the symmetry of this system, some terms cancel out, allowing various higher-order corrections to become dominant. For different boundaries (such as rectangular ones), and for higher-dimensional systems, the behavior will generally be different. In those cases, most of our estimates will scale as the conventional $L^{-1/\nu}$, except perhaps the estimates $p_{c\text{-}c}$ and p_{R_c}. (To employ the latter, R_c must be known, but we have exact values only for rectangular and conformally related two-dimensional systems [29].) The study of these other systems is a subject for future research.

Another approach to measuring p_c is to use periodic rather than open boundary conditions. A partially periodic system in two dimensions is a cylinder, and crossing in this system was studied in Ref. [12]. The fully periodic rectangle is a torus, and the criterion of crossing is replaced by criteria involving the different topologically distinct ways in which clusters can wrap around the boundaries [30]. (Some authors [11,24,31] have also considered the percolation criterion in which a cluster has the full dimension of the lattice along at least one axis but does not necessarily wrap around.) In Ref. [17] we showed that many estimates of p_c on the torus converge a factor L faster than the estimates for the open square—some converging as fast as $L^{-2-1/\nu}$.

In conclusion, it is clear that the convergence of estimates for the critical occupation probability p_c in percolation systems is highly dependent upon the nature of the estimate, as well as the shape and boundary conditions of the system, and that the shrewd use of this fact can allow one to make very accurate estimates of p_c and scaling exponents.

ACKNOWLEDGMENTS

The authors thank L. N. Shchur and A. Aharony for comments and corrections to the manuscript.

APPENDIX: EXACT ENUMERATION RESULTS

In Table II we give the exact expressions for the crossing probability function $R_L(p)$ for site percolation on a square lattice of size $L\times L$, for crossing from one given side of the square to the opposite side (such as left to right). The results for $L=2$ to 5 were given previously by Reynolds *et al.* [2]. Those for $L=6$ and $L=7$ were calculated previously for the work reported in Ref. [5], but reported in a different format [results were given for $R'_L(p)$ rather than $R_L(p)$ itself]. From the results here, one can with reasonable ease calculate the various estimates of p_c given in Table I using a symbolic mathematics program such as MAPLE or MATHEMATICA. A file containing these polynomials in forms readable by such programs is available by email from the authors.

An alternative way to represent these results is as a series in $p^n q^{N-n}$, where $q=1-p$ and $N=L^2$. The transformation can be achieved by substituting $p\to 1/(1+r)$, multiplying by $(1+r)^N p^N$, expanding, and replacing $r\to q/p$. The results are given in Table III.

This is also the form that Reynolds [2] used in their series for $R_2(p)$ to $R_5(p)$. From the present point of view, these series are interesting because they are precisely in the form of Eq. (15), so that the coefficient $c_{L,n}$ of $p^n q^{N-n}$ in $R_L(p,q)$ above is related to the microcanonical crossing probability $R_{L,n}$ simply by

$$R_{L,n}=\frac{c_{L,n}}{\binom{N}{n}}=\frac{c_{L,n}n!(N-n)!}{N!}. \tag{A1}$$

That is, $c_{L,n}$ represents the number of configurations with n occupied sites that satisfy the crossing criterion, out of a total of $\binom{N}{n}$ possible configurations of the n occupied sites among the $N=L^2$ sites of the lattice. For example, of the $16!/(6!10!)=8008$ possible configurations of 6 occupied sites on a 4×4 lattice, exactly 390 are percolating by crossing in one direction [from the third term in $R_4(p,q)$], yielding a microcanonical probability $R_{4,6}=390/8008=0.048\,701\ldots$. Likewise, for $n=16$ occupied sites on the 4×4 system, there is exactly one percolating system out of one total system.

Thus, the polynomials given in Table III represent the microcanonical $R_{L,n}$ for L up to 7.

[1] D. Stauffer and A. Aharony, *Introduction to Percolation Theory,* 2nd ed. (Taylor & Francis, London, 1994).
[2] P. J. Reynolds, H. E. Stanley, and W. Klein, Phys. Rev. B **21**, 1223 (1980).
[3] S. Kirkpatrick, in *Ill Condensed Matter*, Proceedings of the Les Houches Summer School, edited by R. Balian, R. Maynard, and G. Toulouse (North-Holland, Amsterdam, 1979).
[4] A. P. Young and R. B. Stinchcombe, J. Phys. C **8**, L535 (1975).
[5] R. M. Ziff, Phys. Rev. Lett. **69**, 2670 (1992).
[6] F. Yonezawa, S. Sakamoto, and M. Hori, Phys. Rev. B **40**, 636 (1989).
[7] R. P. Langlands, C. Pichet, P. Pouliot, and Y. Saint-Aubin, J. Stat. Phys. **67**, 553 (1992).
[8] R. P. Langlands, P. Pouliot, and Y. Saint-Aubin, Bull. Am. Math. Soc. **30**, 1 (1994).
[9] R. M. Ziff, Phys. Rev. E **45**, 2547 (1996).
[10] A. Aharony and J.-P. Hovi, Phys. Rev. Lett. **72**, 1941 (1994).
[11] C.-K. Hu, C.-Y. Lin, and J.-A. Chen, Phys. Rev. Lett. **75**, 193 (1995).
[12] J.-P. Hovi and A. Aharony, Phys. Rev. E **53**, 235 (1996).
[13] D. Stauffer, Phys. Lett. A **83**, 404 (1981).
[14] J. Adler, M. Moshe, and V. Privman, Phys. Rev. B **26**, 1411 (1982).
[15] J. Adler, M. Moshe, and V. Privman, Ann. Isr. Phys. Soc. **5**, 397 (1983).
[16] M. E. J. Newman and R. M. Ziff, Phys. Rev. Lett. **85**, 4104 (2000).
[17] M. E. J. Newman and R. M. Ziff, Phys. Rev. E **64**, 016706 (2001).
[18] C.-K. Hu, Phys. Rev. B **46**, 6592 (1992).

[19] H. Gould and J. Tobochnik, *An Introduction to Computer Simulation Methods*, 2nd ed. (Addison-Wesley, Reading, MA, 1996), p. 444.
[20] J. E. de Freitas, L. S. Lucena, and S. Roux, Physica A **266**, 81 (1999).
[21] L. N. Shchur and O. A. Vasilyev, e-print cond-mat/0005448.
[22] R. E. Tarjan, J. Assoc. Comput. Mach. **22**, 215 (1975).
[23] N. Jan, T. Lookman, and D. Stauffer, J. Phys. A **16**, L117 (1983).
[24] J. Machta, Y. S. Choi, A. Lucke, T. Schweizer, and L. M. Chayes, Phys. Rev. E **54**, 1332 (1996).
[25] R. M. Ziff, Comput. Phys. **12**, 385 (1998). An implementation of this random number generator is available as the subroutine GSL_RNG_GFSR4 in the GNU scientific library, available from http://sources.redhat.com/gsl/ref/gsl-ref_10.html.
[26] R. M. Ziff, Phys. Rev. Lett. **72**, 1942 (1994).
[27] T. W. Burkhardt, Z. Phys. B: Condens. Matter **39**, 159 (1980).
[28] C.-K. Hu, C.-N. Chen, and F. Y. Wu, J. Stat. Phys. **82**, 1199 (1996).
[29] J. L. Cardy, J. Phys. A **25**, L201 (1992).
[30] H. T. Pinson, J. Stat. Phys. **75**, 1167 (1994).
[31] C.-K. Hu, Phys. Rev. Lett. **76**, 3875 (1996).
[32] In fact, Hovi and Aharony found that the data for p_{av} in their Fig. 1 could be fit best using a value of $\omega \simeq 0.90$, but for the data of their Fig. 5 $\omega = 0.85$ gave the better fit.